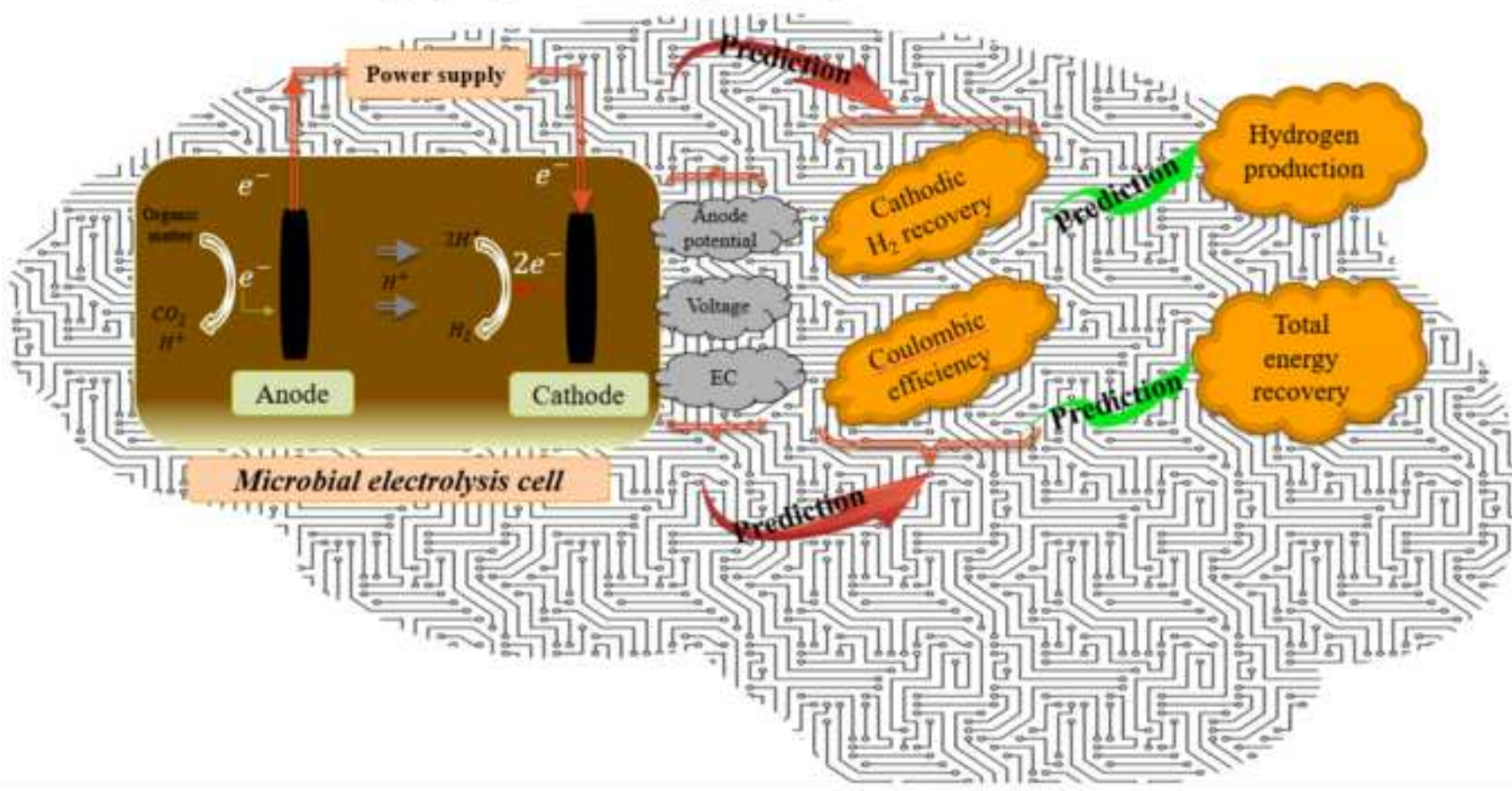


Elsevier required licence: © <2020>. This manuscript version is made available under the CC-BY-NC-ND 4.0 license <http://creativecommons.org/licenses/by-nc-nd/4.0/>
The definitive publisher version is available online at
[\[https://www.sciencedirect.com/science/article/abs/pii/S0960852420312396?via%3Dihub\]](https://www.sciencedirect.com/science/article/abs/pii/S0960852420312396?via%3Dihub)

Modelling hydrogen and energy recovery in MEC with ANFIS and ANN



Highlights

- ANN and ANFIS models were developed for H₂ and total energy recoveries in MEC
- ANFIS models showed better prediction strengths than ANN models
- Voltage and EC were key factors for predicting H₂ recovery and coulombic efficiency
- Coulombic efficiency and r_{cat} showed similar importance in H₂ and energy recoveries

1
2
3
4
5
6
7
8
9
10
11
12
13
14
15
16
17
18
19
20
21
22
23
24
25
26
27
28
29
30
31
32
33
34
35
36
37
38
39
40
41
42
43
44
45
46
47
48
49
50
51
52
53
54
55
56
57
58
59
60
61
62
63
64
65

Effective modelling of hydrogen and energy recovery in microbial electrolysis cell by artificial neural network and adaptive network-based fuzzy inference system

Ahmad Hosseinzadeh^a, John L. Zhou^{a*}, Ali Altaee^a, Mansour Baziar^b, Donghao Li^c

^a Centre for Green Technology, School of Civil and Environmental Engineering, University of Technology Sydney, NSW 2007, Australia

^b Ferdows School of Paramedical and Health, Birjand University of Medical Sciences, Birjand, Iran

^c Department of Chemistry, MOE Key Laboratory of Biological Resources of Changbai Mountain & Functional Molecules, Yanbian University, Yanji 133002, Jilin Province, PR China

*Correspondence author:

Prof John L. Zhou, email: Junliang.zhou@uts.edu.au

Abstract

1 This study aims to analyze and model cathodic H₂ recovery (r_{cat}), coulombic efficiency (CE)
2
3 with inputs of voltage, electrical conductivity (EC) and anode potential, and H₂ production
4
5 rate and total energy recovery with inputs of r_{cat} and CE in a microbial electrolysis cell using
6
7 artificial neural network (ANN) and adaptive network-based fuzzy inference system (ANFIS)
8
9 procedures. Both ANN and ANFIS models demonstrated great goodness of fit for r_{cat} , CE, H₂
10
11 production rate and total energy recovery prediction with high R^2 values. The sum square
12
13 error values for r_{cat} (0.0017), CE (0.0163), H₂ production rate (0.1062) and total energy
14
15 recovery (0.0136) in ANN models were slightly higher than those in ANFIS models at
16
17 0.0005, 0.0091, 0.1247 and 0.0148 respectively. Sensitivity analysis by ANN models
18
19 demonstrated that voltage, EC, r_{cat} and r_{cat} were the most effective factors for r_{cat} , CE, H₂
20
21 production rate and total energy recovery, respectively.
22
23
24
25
26
27
28
29

30 Keywords: ANN; ANFIS; Bio-hydrogen; Machine learning; MEC; Modelling
31
32
33
34
35
36
37
38
39
40
41
42
43
44
45
46
47
48
49
50
51
52
53
54
55
56
57
58
59
60
61
62
63
64
65

1. Introduction

1 Energy has been the driving force of economic development since industrial revolution. It has
2
3 been estimated that the world will require 57% more energy by 2050 considering 1.1% annual
4
5 growth of world population (Divya Priya et al., 2020). In addition, water scarcity is
6
7 considered as one the most important global concerns (Nouri et al., 2019; Zarei et al., 2020).
8
9 Since natural gas, coal and oil are three of the most important finite sources of the energy at
10
11 present, and global large-scale use of such **fossil fuels** emits many inorganic and organic
12
13 pollutants such as CO, NO_x and carcinogenic polycyclic aromatic hydrocarbons (King et al.,
14
15 2004; Organ et al., 2020), exploring appropriate solutions to tackle these challenges is of great
16
17 responsibilities (Divya Priya et al., 2020; Gielen et al., 2019; Hosseinzadeh et al., 2020b; Mu
18
19 et al., 2020). There are various strategies to manage each of these challenges separately;
20
21 however, development of a technology which simultaneously address all of these challenges,
22
23 is timely and innovative.
24
25
26
27
28
29

30 Microbial fuel cell (MFC) and microbial electrolysis cell (MEC) are regarded as two
31
32 rewarding technologies in which electroactive microorganisms use the organic matter to
33
34 produce energy (Cario et al., 2019; Gandu et al., 2020; Jiang et al., 2020). There are two
35
36 common configurations for these processes either as single or dual chamber, in both of which
37
38 two electrodes as anode and cathode are installed and electrically connected by an external
39
40 circuit. In anode chamber, the electron reducing bacteria oxidizing the organic matter donate
41
42 electron to the anode through three different methods including direct electron transfer,
43
44 electron transfer through the membrane proteins of the bacteria e.g. nanowires, through
45
46 soluble mediators, which are present in electrolyte (Cui et al., 2015; Logan et al., 2006). High
47
48 electrical conductivity (EC) of the electrolyte simplifies the electron transfer and reduces
49
50 internal resistance resulting in greater energy recovery (Lefebvre et al., 2012). However, there
51
52 is limited information regarding the importance of EC in comparison to the other factors and
53
54 the simultaneous effect of EC on cathode recovery and Coulombic efficiency (CE), and the
55
56
57
58
59
60
61
62
63
64
65

1 behavior of the separate parts of the MEC at different levels of EC. CE is defined as the ratio
2 of the potential electrons which can be drawn from the substrate and transferred to the anode
3 per the actual ones (Tang et al., 2014). Operating conditions specially the level of anode
4 potential have great importance in selection of the types of the microbial communities
5 activating on anode surface as oxidizers and affecting the CE, and consequently, the energy
6 recovery (Chou et al., 2014). The ratio of the actual recovered H₂ moles to the possible ones
7 according to the measured current is regarded as the cathodic H₂ recovery which can be
8 affected by different factors such as resistance which can be affected by EC (Call and Logan,
9 2008). The outputs of the MEC systems are usually determined by the hydrogen production
10 rate in MEC, and total energy recovery (Call and Logan, 2008). CE and cathodic H₂ recovery
11 directly affect both of these parameters, yet there is no study in this regard. In addition, there
12 is information deficiency on the importance of CE and cathodic H₂ recovery in energy
13 efficiency of MECs. In order to enhance the performances of such processes, operating
14 process at optimum condition is regarded as one of the plausible options, which is frequently
15 neglected. There are two strategies using modelling or laboratory experiments to optimize
16 such processes, and modelling is much cheaper and faster than the laboratory experiments
17 (Pinto et al., 2012). Therefore, with optimization of this process, it is potentially able to
18 alleviate water scarcity, produce energy and reduce environmental pollution simultaneously.
19 In addition, the determination of the most effective part of the process as well as the
20 importance of the variables in process will be crucial to optimize and improve the efficiency
21 of processes.

22 Artificial neural network (ANN), which is inspired from the structure of the human brain,
23 is considered as one of the promising procedures to master different types of correlations
24 existing between various dependent and independent variables. To learn these correlations,
25 ANN procedure does not need to fully comprehend the mechanistic nature and the
26 mathematical background of the processes (Hosseinzadeh et al., 2020a; Rego et al., 2018).

1
2
3
4
5
6
7
8
9
10
11
12
13
14
15
16
17
18
19
20
21
22
23
24
25
26
27
28
29
30
31
32
33
34
35
36
37
38
39
40
41
42
43
44
45
46
47
48
49
50
51
52
53
54
55
56
57
58
59
60
61
62
63
64
65

However, adaptive neuro-fuzzy inference system (ANFIS) developed by Jang (1993) combines the ANN learning abilities with the capabilities of fuzzy logic systems for uncertainty explanation (Betiku et al., 2016). Since the performances of these two machine learning models are dependent upon the type of the applications, there are diverse applications of simultaneously using these procedures in various fields (Betiku et al., 2016; Dastorani et al., 2010; Entchev and Yang, 2007; Hosseinzadeh et al., 2020b; Izadi et al., 2019; Mehdizadeh et al., 2016). However, there was no study which used these two models in MEC processes. Since these two procedures do not need any detailed knowledge of the process, they can be a promising option for the simulation of the MEC process (Tsompanas et al., 2019).

Using ANN and ANFIS models, this study therefore aims to model the effects of applied voltage, electrical conductivity and anode potential on cathodic H₂ recovery and coulombic efficiency. Secondly, the effects of coulombic efficiency and cathodic H₂ recovery on total energy and cathodic H₂ recoveries using ANN and ANFIS procedures in a single chamber MEC are examined. In addition, the **relative** importance of the effective factors in the output of this process is determined by sensitivity analysis.

2. Materials and methods

2.1. Data collection and processing

To generate sophisticated and rigorous **analyses** of the process, the experimental results of one single chamber reactor were used to develop computer models under **similar conditions** of **buffer solutions**, feeding, configuration of the reactor, electrode type **and composites**. Call and Logan (2008) experimentally studied the effects of applied voltage, EC, anode potential, CE and cathodic H₂ recovery on H₂ production rate and total energy recovery in a single chamber **MEC reactor**. The reported experimental results were extracted by Plot Digitizer. In order to reduce the complexity of the computation and avoid overtraining, the input and output

experimental data were randomized (Sharma et al., 2016) in a range from 0.1 to 0.9 using Eq.

1:
2

3
4 proportion of normalized $x_i = \frac{x_i - \text{minimum value of data}}{\text{maximum value of data} - \text{minimum value of data}} \times (0.9 - 0.1) + 0.1$
5

6 (1)
7
8
9

10 2.2. ANN

11 Four different feed-forward ANN models were developed by MATLAB R2018b to model CE
12 and cathodic H₂ recovery with EC, applied voltage and anode potential as inputs; H₂
13 production rate along with total energy recovery with inputs of CE and cathodic H₂ recovery.
14
15

16 The number of neurons in input and output layers were as same as the number of input and
17 output variables in each model. To determine the appropriate number of neurons in hidden
18 layer, 1 to 20 neurons were loaded over different training approaches to develop many
19 models, among which the most accurate model was selected according to the obtained mean
20 square error (MSE) (Eq. 2), *R*-squared (*R*²) (Eq. 3) and correlation coefficient (*R*) (Eq. 4) in
21 models of all, training, validation and test datasets (Baziar et al., 2017). In this study, 80% of
22 the data (19 data points) was employed to train (13 data points), validate (3 data points) and
23 test (3 data points) the developed models. The remaining 20% of the data (5 data points) was
24 used for additional test. In the first part, 80% of the data was divided into three subdivisions
25 of training, validation and testing datasets with 70%, 15% and 15% consecutively. Gradient
26 descent with momentum (trainngdm), scaled conjugate gradient (trainscg), resilient back-
27 propagation (trainrp) and Levenberg-Marquardt (trainlm) as four various backpropagation
28 training algorithms were employed to select the best training algorithm in modelling of
29 cathodic H₂ recovery, CE, H₂ production rate and total energy recovery. It is worth
30 highlighting that the modelling process was carried out with five repetitions to improve the
31 prediction performances as well as the precisions of the models and diminish the MSE.
32
33
34
35
36
37
38
39
40
41
42
43
44
45
46
47
48
49
50
51
52
53
54
55
56
57
58
59
60
61
62
63
64
65

$$MSE = \frac{1}{N} \sum_{i=1}^N (y_{prd,i} - y_{Act,i})^2 \quad (2)$$

$$R^2 = 1 - \frac{\sum_{i=1}^N (y_{prd,i} - y_{Act,i})}{\sum_{i=1}^N (y_{prd,i} - y_m)} \quad (3)$$

$$R_{xy} = \frac{\sum (x_i - \bar{x})(y_i - \bar{y})}{\sqrt{(\sum (x_i - \bar{x})^2) \sum (y_i - \bar{y})^2}} \quad (4)$$

2.3. ANFIS

ANFIS, which is a combination of the ANN learning ability and fuzzy logic systems reasoning capability, with six layers of output, total output, defuzzy, product and normalized, fuzzy and input was applied to model the response variables. In contrast to the fuzzy and defuzzy layers in which the adaptive nodes are variable and are determined at the train phase, the number of nodes in remainder layers are steady. The training approach is similar to that in the ANN models (Souza et al., 2018).

The Gaussian (*gaussmf*), trapezoidal (*trapmf*), difference between two sigmoidal (*dsigmf*), generalized bell-shaped (*gbellmf*), Gaussian combination (*gauss2mf*), and triangular (*trimf*) membership function (MF) in the function *genfis1* of the MATLAB R2018b were used to construct the system of fuzzy inference for ANFIS. The least square estimations coupled with the back-propagation algorithms were combined together and employed to model the process as a hybrid optimization approach (Souza et al., 2018).

2.4. Comparison between ANFIS and ANN models

In order to evaluate and compare the precision of the developed ANFIS and ANN models, four indices including determination coefficient (R^2) (Eq. 3), adjusted- R^2 ($adj-R^2$) (Eq. 5), sum squared error (SSE) (Eq. 6) and root mean square error (RMSE) (Eq. 7) were employed. In principle, the lower the values of the MSE, SSE and RMSE and the higher the values of the R^2 and $adj-R^2$, the higher the precision and goodness of fit of the model (Hosseinzadeh et al.,

2018; Hosseinzadeh et al., 2020b). It should be stressed that all of the extracted data were used to compare the developed models.

$$R^2_{adjusted} = 1 - \frac{(1-R^2)(N-1)}{N-p-1} \quad (5)$$

$$SSE = \sum_{i=1}^N (y_{prd,i} - y_{exp,i})^2 \quad (6)$$

$$RMSE = \sqrt{\frac{1}{N} \sum_{i=1}^N (y_{prd,i} - y_{Act,i})^2} \quad (7)$$

where $y_{prd,i}$ and $y_{Act,i}$ are the predicted and actual proportions of dependent variables (outputs), consecutively; y_m and N are the mean of actual proportion of dependent variables and the total number of data points, respectively.

2.5. Sensitivity analysis

An equation-based approach (Eq. 8) as sensitivity analysis firstly presented by Garson (Hosseinzadeh et al., 2020b), was used to determine the importance portion of the various effective factors on the response factors. In ANN models developed, the effective portions of the EC, applied voltage and anode potential on the CE% and cathodic H₂ recovery, and the effective portions of the CE% and cathodic H₂ recovery on H₂ production rate and total energy recovery were evaluated in a MEC process.

$$I_j = \frac{\sum_{m=1}^{N_h} \left(\left(\frac{|W_{jm}^{ih}|}{\sum_{k=1}^{N_i} |W_{km}^{ih}|} \right) \times |W_{mn}^{ho}| \right)}{\sum_{k=1}^{N_i} \left\{ \sum_{m=1}^{N_h} \left(\frac{|W_{km}^{ih}|}{\sum_{k=1}^{N_i} |W_{km}^{ih}|} \right) \times |W_{mn}^{ho}| \right\}} \times 100 \quad (8)$$

where I_j is the importance of the input, N_h and N_i are the proportion of the hidden layer neuron and proportion of independent variables consecutively; W , h , i and o are related to ANN weight, hidden, input and output layers correspondingly; the n , m and k are the neuron number of the output, hidden and input layers respectively (Hosseinzadeh et al., 2020a).

To assess the importance of the independent variables in dependent variables in ANFIS models developed, six single factor models were built for each of the EC, anode potential,

1 applied voltage with both of CE% and cathodic H₂ recovery under the best conditions
2 obtained, and four other single factor models were developed for each of CE% and cathodic
3 H₂ recovery with H₂ production rate and total energy recovery.
4
5
6
7

8 **3. Results and discussion**

9 10 *3.1. ANN models for CE, cathodic H₂ recovery, H₂ production and energy recovery*

11 12 *3.1.1. Selection of backpropagation training algorithm*

13 Normally the higher proportions of the correlation coefficient (R) as well as the lower
14 proportions of the MSE, the greater strength of the training algorithms (Jacob and Banerjee,
15 2016; Zhao et al., 2019). With respect to the results obtained, Levenberg-Marquardt was
16 selected as the best training algorithm for CE, cathodic H₂ recovery, H₂ production rate and
17 total energy recovery training processes.
18
19
20
21
22
23
24
25
26

27 *3.1.2. Neuron number optimization*

28 According to the best developed model in best training algorithm, a neuron with smallest
29 MSE in all data (train, validation and test data) was chosen as the best neuron number
30 (Elmolla et al., 2010). Based on the developed models, the neurons 7, 7, 11 and 17 were
31 selected as the best for cathodic H₂ recovery, CE, H₂ production rate and total energy
32 recovery respectively. Finally, the obtained appropriate topologies were 3-7-1 and 3-7-1 for
33 cathodic H₂ recovery and CE consecutively. In addition, 2-11-1 and 2-17-1 were selected as
34 the best topologies for H₂ production rate and total energy recovery correspondingly. It is
35 worth highlighting that the first and last number in each topology demonstrate the number of
36 independent and dependent variables in each model.
37
38
39
40
41
42
43
44
45
46
47
48
49
50
51

52 *3.1.3. Validation and testing of the models*

53 Two 15% of the train datasets which was 80% of the all data were used to validate and test
54 the developed models. The ANN model used for prediction of the cathodic H₂ recovery and
55 CE are presented in Eq. 9, and that of the H₂ production rate and the total energy recovery is
56
57
58
59
60
61
62
63
64
65

presented in Eq. 10. Figs 1 and 2 demonstrate the scattergrams with correlation coefficients of all data (train, validation and test data) in one graph, and their residual errors for the cathodic H₂ recovery, CE, H₂ production rate and total energy recovery models consecutively.

$$ANN \text{ equation} = Purelin(LW \times tansig(IW \times [Voltage; EC; anode \text{ potential}] + b_1) + b_2) \quad (9)$$

$$ANN \text{ equation} = Purelin(LW \times tansig(IW \times [Cathodic H_2 \text{ recovery}; CE] + b_1) + b_2) \quad (10)$$

As can be seen in Figs 1a and 1b, the values of parameter R for cathodic H₂ recovery and CE were 0.9994 and 0.9985 respectively, while R values for the H₂ production rate and total energy recovery were 0.9441 and 0.9939. In addition, the MSE values of these four models were 0.0001, 0.0001, 0.0073 and 0.004 respectively.

Based on the built models, the cathodic H₂ recovery, CE, H₂ production rate and total energy recovery in the single chamber MEC can be predicted up to 99.83%, 98.19%, 87.05% and 98.07%. The best liner fit equations of the developed models for the cathodic H₂ recovery, CE, H₂ production rate and total energy recovery are presented in equations 11-14 correspondingly.

$$y = 1.0037 x - 0.0077 \quad (R^2 = 0.9983) \quad (11)$$

$$y = 1.0132 x - 0.0027 \quad (R^2 = 0.9819) \quad (12)$$

$$y = 0.7285 x + 0.1278 \quad (R^2 = 0.8705) \quad (13)$$

$$y = 0.9171 x + 0.0605 \quad (R^2 = 0.9807) \quad (14)$$

Moreover, additional tests were carried out to check the strengths of the developed ANN models in prediction of the response variables. According to the findings of the additional tests, the paired values of the R^2 and MSE parameters were 0.9988 and 0.0002 for cathodic H₂ recovery, 0.9356 and 0.0029 for CE, 0.8469 and 0.0132 for H₂ production rate, and 0.9940

and 0.0023 for total energy recovery. Fig. 3 depicts both actual and predicted values of the outputs in additional tests for all ANN models.

Tsompanas et al. (2019) showed a great capability of the ANN models for an MFC system. The production of voltage with inputs of cathode size, electrodes location, cylinder materials and logarithmic value of load resistance was modelled with R^2 of 0.9932. Furthermore, Jaeel et al. (2016) constructed an ANN model for power generation in an MFC with inputs of anode inclined angle, flow rate and time. The developed model with topology of 3-16-1 and R^2 of 0.99889 could mimic well the actual data (Jaeel et al., 2016). Moreover, Sewsynker et al. (2015) applied five ANNs with topologies of 6-(6, 8, 11, 12, 14)-1 to model the H_2 production in MECs, and they reported average R^2 values of 0.85. Therefore, the application of ANN model in this and other research indicated the great potential of this procedure for process modelling.

3.2. ANFIS models for cathodic H_2 recovery, CE, H_2 production rate and total energy recovery

The Sugeno fuzzy inference system (FIS) structure showing superior strength than the Mamdani FIS was used to model the cathodic H_2 recovery, CE, H_2 production rate and total energy recovery in a single chamber MES process. In addition, the hybrid approach for optimization of the neural networks was used to model all outputs.

In this work, all data were divided into 80% for training and 20% for testing. The results of ANFIS models including prediction of the outputs in train and test phases for cathodic H_2 recovery, CE, H_2 production rate and total energy recovery models are depicted in Fig. 4, and their residual errors are displayed in Fig. 5. The MSE values for the cathodic H_2 recovery models are 0.0001 and 3.7013×10^{-8} in training and 0.0001 and 0.0016 in testing, and their R^2 are 1 and 0.9834 in training and 0.9972 and 0.9858 in testing. In comparison, the MSE values for H_2 production rate and the total energy recovery models were 0.0057 and 0.0105 in

1 training and 0.0004 and 0.0016 in testing, with the R^2 values of 0.9000 and 0.9870 in training
2 and 0.9785 and 0.9864 in testing datasets. At each epoch, the generalization capacity of the
3 FIS was evaluated using the testing datasets. It is worth highlighting that the error sizes in
4 ANFIS are demonstrative of mapping function compatibility and differences among the actual
5 and predicted values of the outputs. The factors of the membership function were regulated to
6 construct an appropriate goodness of fit for the predicted values of the response variables and
7 the experimental ones.
8

9
10
11 In order to improve ANFIS models, six various MFs including trapezoidal (trapmf),
12 difference between two sigmoidal (dsigmf), generalized bell-shaped (gbellmf), Gaussian
13 combination (gauss2mf), Gaussian (gaussmf) and triangular (trimf) were employed.
14

15
16 According to the developed models, trimf was chosen as the best MF for the ANFIS models
17 developed for cathodic H_2 recovery, CE, H_2 production rate and total energy recovery. The
18 results of the developed ANFIS models for all four outputs were assessed under linear states.
19
20 Table 1 presents the attained results for ANFIS models of cathodic H_2 recovery, CE, H_2
21 production rate and total energy recovery under different MFs.
22

23
24 As is evident in Table 1, the trimf from the approach of hybrid optimization with linear
25 output was the best membership function for all of the cathodic H_2 recovery, CE, H_2
26 production rate and total energy recovery. In addition, a great dependence between the errors
27 in train and test phases, membership functions and the approach of the optimization can be
28 observed.
29

30
31 Zareei and Khodaei (2017) applied ANFIS to model the biogas production from maize
32 straw and cow manure with inputs of stirring intensity of the substrates, total solid content and
33 C/N ratio. The obtained R^2 for the developed ANFIS model was 0.99 (Zareei and Khodaei,
34 2017) indicating high strength of the ANFIS models in various processes, being in agreement
35 with the present study. In addition, Sargolzaei et al. (2012) modeled the flux and rejection of
36 a membrane by ANFIS, in which flow rate, temperature, pH and feed COD concentration
37

1 were considered as the inputs. The obtained average testing errors of the membrane flux and
2 membrane rejection were 0.00215 and 0.00204, respectively demonstrating the high strength
3 of the ANFIS models (Sargolzaei et al., 2012). Thus, the high capability of the ANFIS model
4 for simulating various processes has been shown.
5
6
7
8
9

10 *3.3. Comparison between ANN and ANFIS models*

11 The values of R^2 , $\text{adj-}R^2$, SSE and RMSE were employed to compare the goodness of fit and
12 accuracy of the constructed ANFIS and ANN models for cathodic H_2 recovery, CE, H_2
13 production rate and total energy recovery prediction. The attained proportions of the
14 mentioned statistical factors are listed in Table 2. Furthermore, the experimental and predicted
15 proportions of the outputs are displayed in Figs 1, 3 and 4.
16
17
18
19
20
21
22
23
24

25 According to the obtained $\text{Adj-}R^2$ and R^2 , all of the developed ANFIS models showed
26 slightly better performance than the ANN. For example, the ANFIS models of the cathodic H_2
27 recovery and CE generated lower RMSE and SSE values than the ANN models; however,
28 such error indices for H_2 and total energy recoveries were slightly higher than those of the
29 ANN models. Overall, both of the predictions from ANFIS and ANN models for cathodic H_2
30 recovery, CE, H_2 production and total energy recovery mimicked well with the actual data.
31 The demonstrated performances of the ANN and ANFIS models in the present study are in
32 good agreement with the study of Rego et al. (2018), in which both ANFIS and ANN well
33 modeled the contents of lignin, glucose, xylose and oxidized lignin of sugarcane bagasse in
34 the process of sugarcane bagasse delignification. In addition, the ANFIS models showed
35 better performance than the ANN only for xylose prediction (Rego et al., 2018).
36
37
38
39
40
41
42
43
44
45
46
47
48
49
50
51
52
53

54 *3.4. Model sensitivity analysis*

55 The effective portion of the input variables on outputs have been determined based on the
56 connection weights of the variables in the developed ANN models. In more detail, the
57
58
59
60
61
62
63
64
65

effective portion of the voltage, EC and anode potential on cathodic H₂ recovery and CE;

also, the effective portion of the cathodic H₂ recovery and CE on H₂ production rate and total energy recovery were analyzed by this procedure. The attained weights for the cathodic H₂ recovery, CE, H₂ production rate and total energy recovery networks were listed in Tables 3-6 respectively.

The importance of the input variables in cathodic H₂ recovery, CE, H₂ production rate and total energy recovery models is displayed in Fig 6. As shown, the most effective parameter in cathodic H₂ recovery was the applied voltage with 47% and the next parameters with decreasing order were EC (28%) and anode potential (25%). Whilst, the most efficient parameter for the CE was EC with 41%, and applied voltage and anode potential were ranked next with 35% and 24% effectiveness, respectively. For the H₂ production rate and the total energy recovery, both of the input variables demonstrated approximately equal importance; however, the cathodic H₂ recovery effect on both of these models was slightly more with 51% and 53% consecutively. Similarly, in modeling H₂ production by MECs, Sewsynker et al. (2015) conducted the sensitivity analysis against the substrate type, voltage, concentration of the substrate, pH, configuration of the reactor and temperature which were found to be the most efficient factors in declining order.

4. Conclusions

This work analyzed and modeled four MEC outputs including cathodic H₂ recovery (r_{cat}), CE, H₂ production and total energy recovery by ANN and ANFIS approaches. Voltage, EC and anode potential were the inputs of r_{cat} and CE models, and two outputs (r_{cat} and CE) were applied as the inputs for H₂ production and total energy recovery. All four ANFIS models demonstrated slightly better performance than ANN models. Additionally, sensitivity analysis showed voltage with 47% importance for r_{cat} , EC with 41% importance for CE, and r_{cat} with 51% importance for both H₂ production and 53% for total energy recovery.

Acknowledgments

The authors acknowledge the support from the University of Technology Sydney (UTS) for UTS President's Scholarship and an International Research Scholarship, and a grant from the 111 Project (D18012).

References

1. Baziar, M., Azari, A., Karimaei, M., Gupta, V.K., Agarwal, S., Sharafi, K., Maroosi, M., Shariatifar, N., Dobaradaran, S. 2017. MWCNT-Fe₃O₄ as a superior adsorbent for microcystins LR removal: Investigation on the magnetic adsorption separation, artificial neural network modeling, and genetic algorithm optimization. *Journal of Molecular Liquids*, **241**, 102-113.
2. Betiku, E., Odude, V.O., Ishola, N.B., Bamimore, A., Osunleke, A.S., Okeleye, A.A. 2016. Predictive capability evaluation of RSM, ANFIS and ANN: A case of reduction of high free fatty acid of palm kernel oil via esterification process. *Energy Conversion and Management*, **124**, 219-230.
3. Call, D., Logan, B.E. 2008. Hydrogen production in a single chamber microbial electrolysis cell lacking a membrane. *Environmental Science & Technology*, **42**(9), 3401-3406.
4. Cario, B.P., Rossi, R., Kim, K.-Y., Logan, B.E. 2019. Applying the electrode potential slope method as a tool to quantitatively evaluate the performance of individual microbial electrolysis cell components. *Bioresource Technology*, **287**, 121418.
5. Chou, T.-Y., Whiteley, C.G., Lee, D.-J. 2014. Anodic potential on dual-chambered microbial fuel cell with sulphate reducing bacteria biofilm. *International Journal of Hydrogen Energy*, **39**(33), 19225-19231.
6. Cui, H.-F., Du, L., Guo, P.-B., Zhu, B., Luong, J.H.T. 2015. Controlled modification of carbon nanotubes and polyaniline on macroporous graphite felt for high-performance microbial fuel cell anode. *Journal of Power Sources*, **283**, 46-53.

- 1
2
3
4
5
6
7
8
9
10
11
12
13
14
15
16
17
18
19
20
21
22
23
24
25
26
27
28
29
30
31
32
33
34
35
36
37
38
39
40
41
42
43
44
45
46
47
48
49
50
51
52
53
54
55
56
57
58
59
60
61
62
63
64
65
7. Dastorani, M.T., Moghadamnia, A., Piri, J., Rico-Ramirez, M. 2010. Application of ANN and ANFIS models for reconstructing missing flow data. *Environmental Monitoring and Assessment*, **166**(1-4), 421-434.
8. Divya Priya, A., Deva, S., Shalini, P., Pydi Setty, Y. 2020. Antimony-tin based intermetallics supported on reduced graphene oxide as anode and MnO₂@rGO as cathode electrode for the study of microbial fuel cell performance. *Renewable Energy*, **150**, 156-166.
9. Elmolla, E.S., Chaudhuri, M., Eltoukhy, M.M. 2010. The use of artificial neural network (ANN) for modeling of COD removal from antibiotic aqueous solution by the Fenton process. *Journal of Hazardous Materials*, **179**(1), 127-134.
10. Entchev, E., Yang, L. 2007. Application of adaptive neuro-fuzzy inference system techniques and artificial neural networks to predict solid oxide fuel cell performance in residential microgeneration installation. *Journal of Power Sources*, **170**(1), 122-129.
11. Gandu, B., Rozenfeld, S., Ouaknin Hirsch, L., Schechter, A., Cahan, R. 2020. Immobilization of bacterial cells on carbon-cloth anode using alginate for hydrogen generation in a microbial electrolysis cell. *Journal of Power Sources*, **455**, 227986.
12. Gielen, D., Boshell, F., Saygin, D., Bazilian, M.D., Wagner, N., Gorini, R. 2019. The role of renewable energy in the global energy transformation. *Energy Strategy Reviews*, **24**, 38-50.
13. Hosseinzadeh, A., Baziar, M., Alidadi, H., Zhou, J.L., Altaee, A., Najafpoor, A.A., Jafarpour, S. 2020a. Application of artificial neural network and multiple linear regression in modeling nutrient recovery in vermicompost under different conditions. *Bioresource Technology*, **303**, 122926.
14. Hosseinzadeh, A., Najafpoor, A.A., Jafari, A.J., Jazani, R.K., Baziar, M., Bargozin, H., Piranloo, F.G. 2018. Application of response surface methodology and artificial neural network modeling to assess non-thermal plasma efficiency in simultaneous removal of BTEX from waste gases: Effect of operating parameters and prediction performance. *Process Safety and Environmental Protection*, **119**, 261-270.
15. Hosseinzadeh, A., Zhou, J.L., Altaee, A., Baziar, M., Li, X. 2020b. Modeling water flux in osmotic membrane bioreactor by adaptive network-based fuzzy inference system and artificial neural network. *Bioresource Technology*, **310**, 123391.

16. Izadi, M., Rahimi, M., Beigzadeh, R. 2019. Evaluation of micromixing in helically coiled microreactors using artificial intelligence approaches. *Chemical Engineering Journal*, **356**, 570-579.
17. Jacob, S., Banerjee, R. 2016. Modeling and optimization of anaerobic codigestion of potato waste and aquatic weed by response surface methodology and artificial neural network coupled genetic algorithm. *Bioresource Technology*, **214**, 386-395.
18. Jaeel, A.J., Al-wared, A.I., Ismail, Z.Z. 2016. Prediction of sustainable electricity generation in microbial fuel cell by neural network: Effect of anode angle with respect to flow direction. *Journal of Electroanalytical Chemistry*, **767**, 56-62.
19. Jang, J.S. 1993. ANFIS: adaptive-network-based fuzzy inference system. *IEEE Transactions on Systems, Man, and Cybernetics*, **23**(3), 665-685.
20. Jiang, M., Xu, T., Chen, S. 2020. A mechanical rechargeable small-size microbial fuel cell with long-term and stable power output. *Applied Energy*, **260**, 114336.
21. King, A.J., Readman, J.W., Zhou, J.L., 2004. Dynamic behaviour of polycyclic aromatic hydrocarbons in Brighton Marina, UK. *Marine Pollution Bulletin* **48**, 229-239.
22. Lefebvre, O., Tan, Z., Kharkwal, S., Ng, H.Y. 2012. Effect of increasing anodic NaCl concentration on microbial fuel cell performance. *Bioresource Technology*, **112**, 336-340.
23. Logan, B.E., Hamelers, B., Rozendal, R., Schröder, U., Keller, J., Freguia, S., Aelterman, P., Verstraete, W., Rabaey, K. 2006. Microbial fuel cells: methodology and technology. *Environmental Science & Technology*, **40**(17), 5181-5192.
24. Mehdizadeh, S., Behmanesh, J., Khalili, K. 2016. Comparison of artificial intelligence methods and empirical equations to estimate daily solar radiation. *Journal of Atmospheric and Solar-Terrestrial Physics*, **146**, 215-227.
25. Mu, D., Liu, H., Lin, W., Shukla, P., Luo, J. 2020. Simultaneous biohydrogen production from dark fermentation of duckweed and waste utilization for microalgal lipid production. *Bioresource Technology*, **302**, 122879.

- 1
2
3
4
5
6
7
8
9
10
11
12
13
14
15
16
17
18
19
20
21
22
23
24
25
26
27
28
29
30
31
32
33
34
35
36
37
38
39
40
41
42
43
44
45
46
47
48
49
50
51
52
53
54
55
56
57
58
59
60
61
62
63
64
65
26. Nouri, H., Stokvis, B., Galindo, A., Blatchford, M., Hoekstra, A.Y. 2019. Water scarcity alleviation through water footprint reduction in agriculture: The effect of soil mulching and drip irrigation. *Science of The Total Environment*, **653**, 241-252.
 27. Organ, B., Huang, Y., Zhou, J.L., Yam, Y.S., Mok, W.C., Chan, E.F.C., 2020. Simulation of engine faults and their impact on emissions and vehicle performance for a liquefied petroleum gas taxi. *Science of the Total Environment* **716**, 137066.
 28. Pinto, R.P., Tartakovsky, B., Srinivasan, B. 2012. Optimizing energy productivity of microbial electrochemical cells. *Journal of Process Control*, **22**(6), 1079-1086.
 29. Rego, A.S.C., Valim, I.C., Vieira, A.A.S., Vilani, C., Santos, B.F. 2018. Optimization of sugarcane bagasse pretreatment using alkaline hydrogen peroxide through ANN and ANFIS modelling. *Bioresource Technology*, **267**, 634-641.
 30. Sargolzaei, J., Haghghi Asl, M., Hedayati Moghaddam, A. 2012. Membrane permeate flux and rejection factor prediction using intelligent systems. *Desalination*, **284**, 92-99.
 31. Sewsynker, Y., Kana, E.B.G., Lateef, A. 2015. Modelling of biohydrogen generation in microbial electrolysis cells (MECs) using a committee of artificial neural networks (ANNs). *Biotechnology & Biotechnological Equipment*, **29**(6), 1208-1215.
 32. Sharma, V., Yang, D., Walsh, W., Reindl, T. 2016. Short term solar irradiance forecasting using a mixed wavelet neural network. *Renewable Energy*, **90**, 481-492.
 33. Souza, P.R., Dotto, G.L., Salau, N.P.G. 2018. Artificial neural network (ANN) and adaptive neuro-fuzzy interference system (ANFIS) modelling for nickel adsorption onto agro-wastes and commercial activated carbon. *Journal of Environmental Chemical Engineering*, **6**(6), 7152-7160.
 34. Tang, X., Li, H., Du, Z., Ng, H.Y. 2014. A phosphorus-free anolyte to enhance coulombic efficiency of microbial fuel cells. *Journal of Power Sources*, **268**, 14-18.
 35. Tsompanas, M.-A., You, J., Wallis, L., Greenman, J., Ieropoulos, I. 2019. Artificial neural network simulating microbial fuel cells with different membrane materials and electrode configurations. *Journal of Power Sources*, **436**, 226832.
 36. Zarei, Z., Karami, E., Keshavarz, M. 2020. Co-production of knowledge and adaptation to water scarcity in developing countries. *Journal of Environmental Management*, **262**, 110283.

- 1
2
3
4
5
6
7
8
9
10
11
12
13
14
15
16
17
18
19
20
21
22
23
24
25
26
27
28
29
30
31
32
33
34
35
36
37
38
39
40
41
42
43
44
45
46
47
48
49
50
51
52
53
54
55
56
57
58
59
60
61
62
63
64
65
37. Zareei, S., Khodaei, J. 2017. Modeling and optimization of biogas production from cow manure and maize straw using an adaptive neuro-fuzzy inference system. *Renewable Energy*, **114**, 423-427.
38. Zhao, Z., Lou, Y., Chen, Y., Lin, H., Li, R., Yu, G. 2019. Prediction of interfacial interactions related with membrane fouling in a membrane bioreactor based on radial basis function artificial neural network (ANN). *Bioresource Technology*, **282**, 262-268.

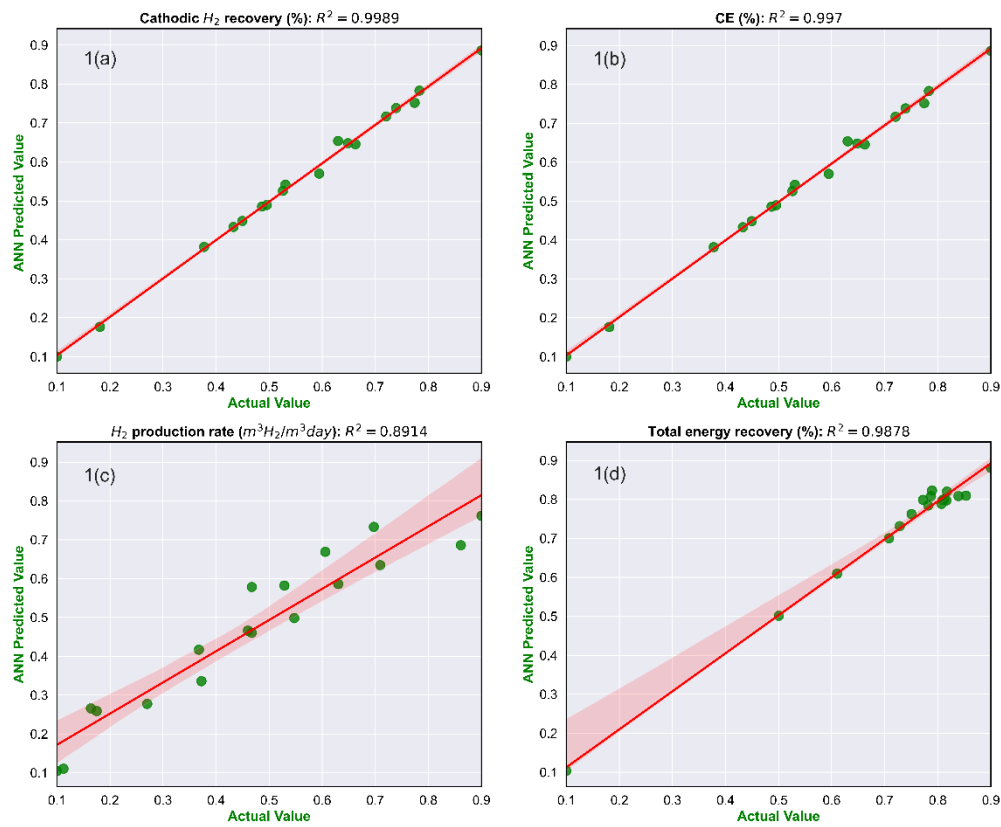


Fig. 1. Correlation coefficients of the developed models by Levenberg-Marquardt training algorithm for (1) cathodic H_2 recovery, (b) CE, (c) H_2 production rate and (d) total energy recovery.

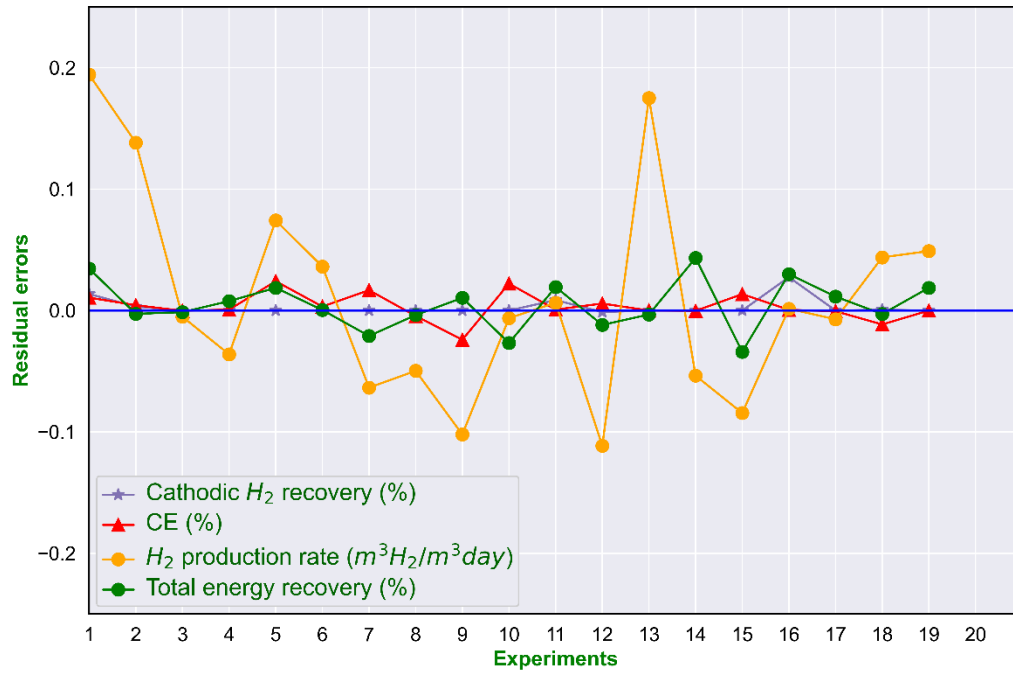


Fig. 2. Residual errors of the developed models by Levenberg-Marquardt training algorithm for (a) cathodic H₂ recovery, (b) CE, (c) H₂ production rate and (d) total energy recovery.

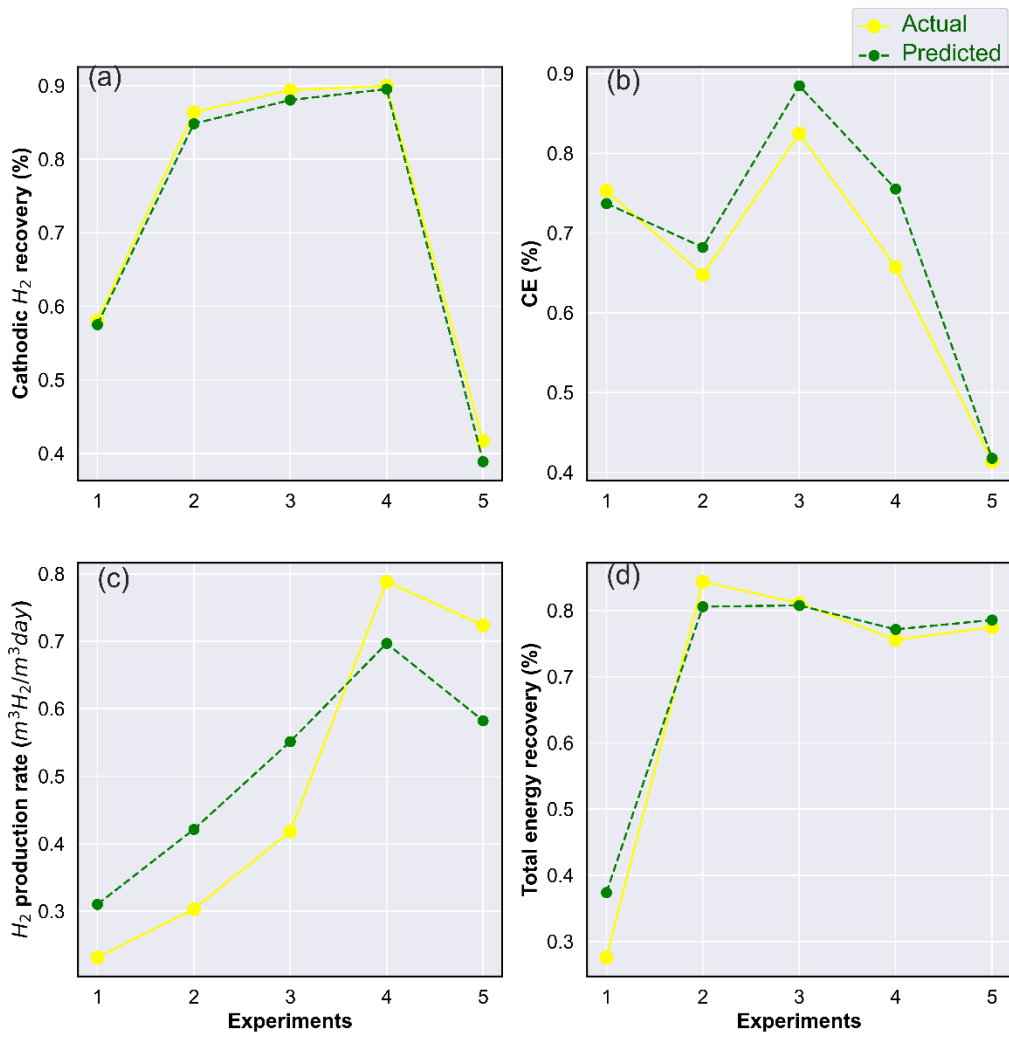


Fig. 3. Additional tests for (a) cathodic H_2 recovery, (b) CE, (c) H_2 production rate, and (d) total energy recovery.

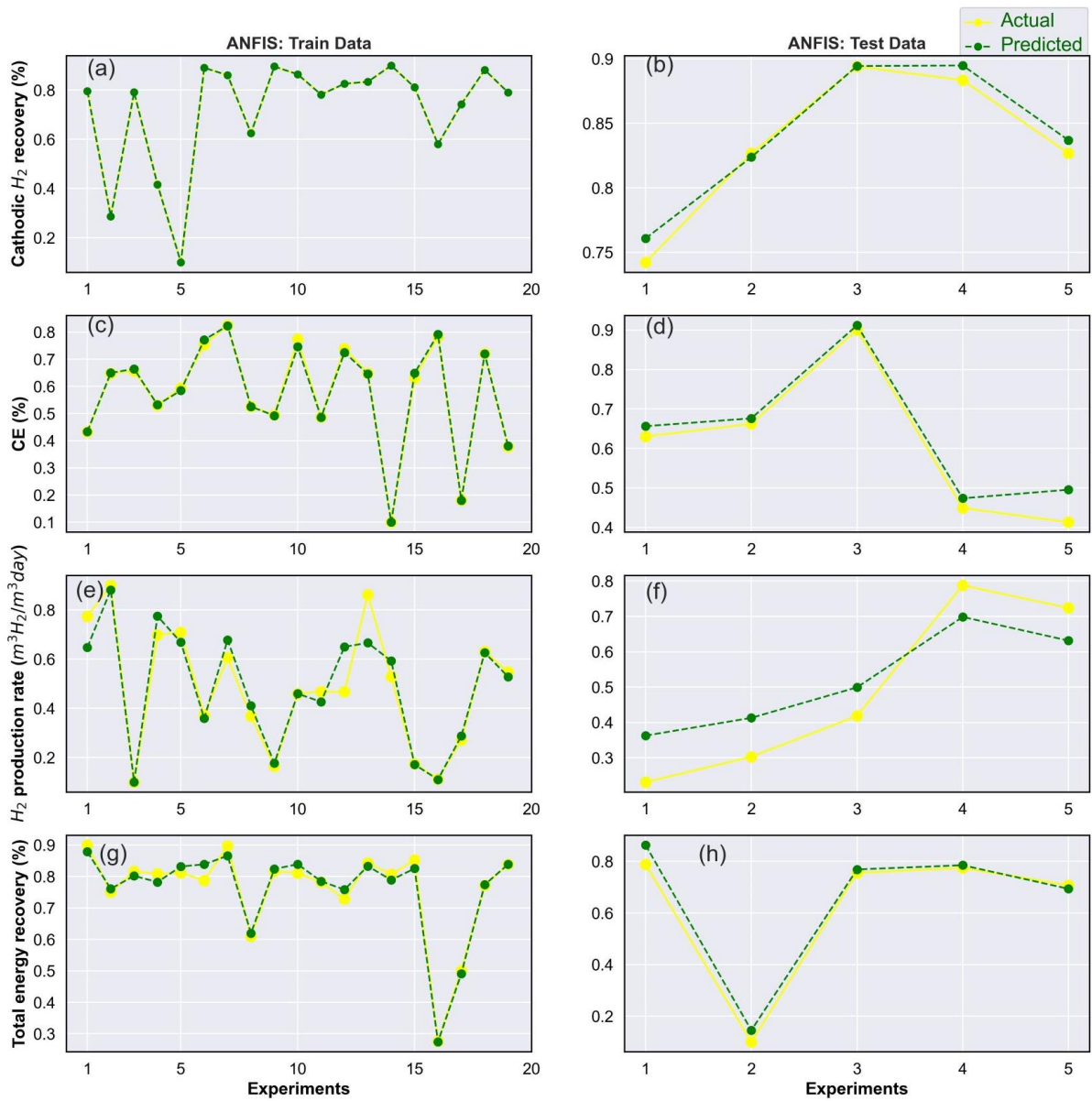


Fig. 4. Actual and predicted values of ANFIS models for (a) training data for cathodic H₂ recovery, (b) test data for cathodic H₂ recovery, (c) training data for CE, (d) test data for CE, (e) training data for H₂ production rate, (f) test data for H₂ production rate, (g) training data for total energy recovery, (h) test data for total energy recovery.

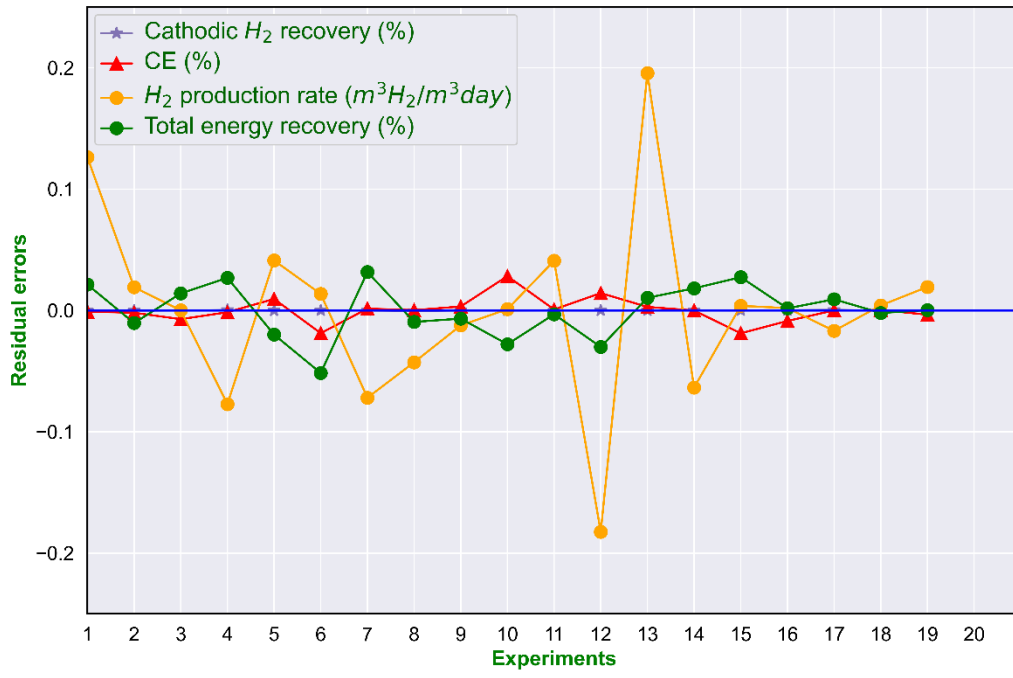


Fig 5. The residual errors of ANFIS models for cathodic H_2 recovery, CE, H_2 production rate and total energy recovery

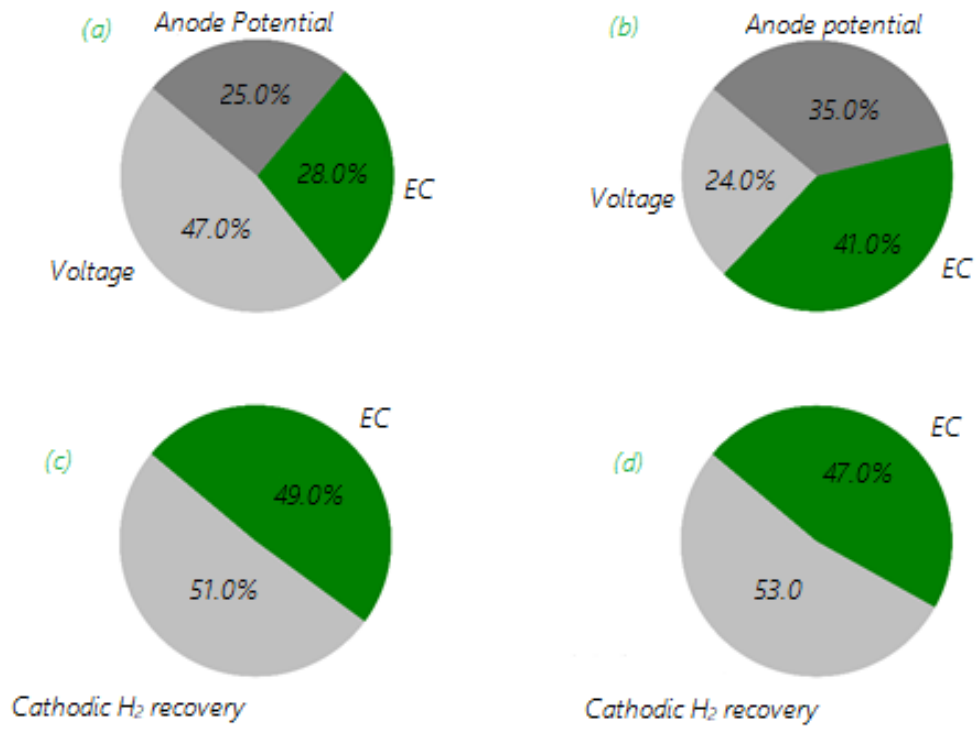


Fig. 6. Percentage importance of the independent factor for (a) cathodic H₂ recovery, (b) CE, (c) H₂ production rate, and (d) total energy recovery.

Table 1

Performance of different membership functions in ANFIS models for cathodic H₂ recovery, CE, H₂ production rate and total energy recovery.

Optimization method	Output model	Model phase	MSE/R	MF type					
				trapmf	trimf	dsigmf	gaussmf	gauss2mf	gbellmf
Hybrid	Linear	Train	MSE	1.27*10 ⁻⁶	3.7*10⁻⁸	3.12*10 ⁻⁸	9.72*10 ⁻⁷	5.006*10 ⁻⁸	1.003*10 ⁻⁸
			(R)	1	1	1	1	1	1
	CHR	Test	MSE	0.0048	1.7*10⁻⁴	0.0154	0.0032	0.0167	0.0216
			(R)	0.9923	0.9917	0.9511	0.9844	0.9495	0.9636
	CE	Train	MSE	1.41*10 ⁻⁴	1.04*10⁻⁴	1.43*10 ⁻⁷	5.13*10 ⁻⁸	1.27*10 ⁻⁸	1.54*10 ⁻⁸
			(R)	0.9976	0.9986	1	1	1	1
		Test	MSE	0.0662	0.0017	0.0013	0.0023	0.0111	0.0036
			(R)	0.9647	0.9929	0.9557	0.9801	0.9585	0.9318
	HPR	Train	MSE	0.0101	0.0058	0.0084	0.0095	0.0103	0.0060
			(R)	0.8850	0.9487	0.9269	0.9143	0.9172	0.9458
		Test	MSE	0.4683	0.0105	0.1310	0.0219	0.1420	0.0195
			(R)	0.8809	0.9936	0.8516	0.8386	0.5449	0.7873
TER	Train	MSE	6.38*10 ⁻⁴	4.56*10⁻⁴	3.89*10 ⁻⁴	3.93*10 ⁻⁴	3.46*10 ⁻⁴	3.4*10 ⁻⁴	
		(R)	0.9893	0.9892	0.9953	0.9929	0.9954	0.9959	
	Test	MSE	0.0027	0.0016	9.21*10 ⁻⁴	0.0221	0.0517	4.09*10 ⁻⁴	
		(R)	0.9953	0.9933	0.9646	0.9617	0.9743	0.9585	

Table 2

Comparison of ANFIS and ANN models for cathodic H₂ recovery, CE, H₂ production rate and total energy recovery.

Statistical index	Cathodic H ₂ recovery		CE		H ₂ production rate		Total energy recovery	
	ANFIS	ANN	ANFIS	ANN	ANFIS	ANN	ANFIS	ANN
	(trimf)	(trainlm)	(trimf)	(trainlm)	(trimf)	(trainlm)	(trimf)	(trainlm)
SSE	0.0005	0.0017	0.0091	0.0163	0.1247	0.1062	0.0148	0.0136
RMSE	0.0049	0.0088	0.0203	0.0272	0.0753	0.0695	0.0259	0.0249
Adj-R ²	0.9994	0.9982	0.9888	0.9811	0.8775	0.8646	0.9800	0.9798
R ²	0.9995	0.9983	0.9892	0.9819	0.8828	0.8705	0.9809	0.9807

Table 3

Weights and biases of the constructed network for the cathodic H₂ recovery.

Neuron	IW			LW	b₁	b₂
	Independent factor			response		
	Voltage	EC	Anode potential			
1	-0.93	1.52	-2.06	-0.44	2.61	-0.5735
2	-2.03	1.41	-0.74	0.23	2.05	
3	2.81	-0.32	-0.30	0.33	-1.36	
4	-2.25	-0.51	1.49	0.14	0.31	
5	0.046	0.98	2.10	-0.06	-1.06	
6	-0.35	-1.72	2.02	-0.40	-2.15	
7	3.61	-0.11	-0.52	1.47	2.98	

Table 4

Weights and biases of the constructed network for CE.

Neuron	IW			LW	b_1	b_2	
	Independent factor						response
	Voltage	EC	Anode potential				
1	-1.58	-1.62	-1.52	1.47	2.72	0.3840	
2	0.10	-2.70	-1.54	-1.77	1.52		
3	-2.17	2.40	0.80	-0.45	0.53		
4	-1.42	-2.31	0.89	-1.04	-0.36		
5	-1.19	-0.41	-2.56	1.02	-1.91		
6	-0.26	3.26	-2.40	-1.80	0.95		
7	0.44	-1.57	-2.17	-0.45	2.64		

Table 5Weights and biases of the constructed network for the H₂ production rate.

Neuron	IW		LW	b ₁	b ₂	
	Independent factor					response
	Cathodic H ₂ recovery	CE				
1	2.20	-4.17	-0.54	-4.60	-0.5264	
2	-3.69	-2.79	0.07	3.64		
3	1.46	-4.41	0.20	-2.77		
4	-3.85	2.97	-1.10	1.90		
5	4.42	1.46	-0.17	-0.90		
6	-1.38	4.52	0.87	-0.50		
7	-2.10	-4.17	0.14	-0.88		
8	-1.62	4.29	-0.21	-1.62		
9	-3.92	2.49	-0.21	-2.79		
10	-3.97	2.41	-0.28	-3.72		
11	4.84	0.34	-0.21	4.41		

Table 6

Weights and biases of the constructed network for the total energy recovery.

Neuron	IW		LW	b_1	b_2	
	Independent factor					response
	Cathodic H ₂ recovery	CE				
1	-0.95	-5.57	0.53	5.86	-0.4391	
2	-5.75	-1.61	-0.04	4.76		
3	0.20	5.76	0.34	-4.62		
4	5.81	0.67	0.02	-3.29		
5	5.25	-2.65	-0.13	-2.71		
6	-5.40	2.30	-0.24	1.92		
7	4.08	4.17	0.32	-1.33		
8	-4.64	-3.42	-0.04	0.65		
9	-5.77	-0.31	-0.10	-0.12		
10	-1.69	-5.52	0.22	-0.60		
11	-4.47	-3.63	0.04	-1.52		
12	4.94	-2.93	0.28	2.22		
13	-4.94	-2.80	0.31	-3.11		
14	4.22	-4.06	-0.05	3.48		
15	4.60	3.49	0.67	4.33		
16	-4.63	3.56	-0.35	-4.95		
17	-2.45	-5.23	0.29	-5.77		

CRedit author statement

Ahmad Hosseinzadeh: investigation, writing - original draft, writing – review and editing

John L. Zhou: supervision, writing – review and editing

Ali Altaee: writing – review and editing

Mansour Baziar: Formal analysis

Donghao Li: writing – review and editing

Declaration of interests

The authors declare that they have no known competing financial interests or personal relationships that could have appeared to influence the work reported in this paper.

The authors declare the following financial interests/personal relationships which may be considered as potential competing interests: